Macromolecules

Article

pubs.acs.org/Macromolecules

# Highly Selective $CO_2$ Capture by Triazine-Based Benzimidazole-Linked Polymers

Ali Kemal Sekizkardes, Suha Altarawneh, Zafer Kahveci, Timur İslamoğlu, and Hani M. El-Kaderi*

Department of Chemistry, Virginia Commonwealth University, 1001 W. Main St., Richmond, Virginia 23284-2006, United States

Supporting Information

**ABSTRACT:** Triazine-based benzimidazole-linked polymers (TBILPs), TBILP-1 and TBILP-2, were synthesized by condensation reaction of 2,4,6-tris(4-formylphenyl)-1,3,5-triazine (TFPT) with 1,2,4,5-benzenetetraamine tetrachloride (BTA) and 2,3,6,7,14,15-hexaaminotriptycene (HATT), respectively. The Ar sorption isotherms at 87 K revealed high surface areas for TBILP-1 (330 $m^2\ g^{-1}$) and TBILP-2 (1080 $m^2\ g^{-1}$). TBILP-2 adsorbed significantly high $CO_2$ (5.19 mmol $g^{-1}$/228 mg $g^{-1}$) at 1 bar and 273 K. Initial slope selectivity calculations demonstrated that TBILP-1 has very high selectivity for $CO_2$ over $N_2$ (63) at 298 K, outperforming all triazine-based porous organic polymers reported to date. On the other hand, the larger surface area of TBILP-2 leads to relatively lower selectivity for $CO_2/N_2$ (40) and $CO_2/CH_4$ (7) at 298 K. TBILPs showed moderate isosteric heats of adsorption for $CO_2$: TBILP-1 (35 kJ $mol^{-1}$) and TBILP-2 (29 kJ $mol^{-1}$) enabling high and reversible $CO_2$ uptake at ambient temperature. In addition, TBILPs displayed promising working capacity, regenerability, and sorbent selection parameter values for $CO_2$ capture from gas mixtures under vacuum swing adsorption (VSA) and pressure swing adsorption (PSA) conditions.

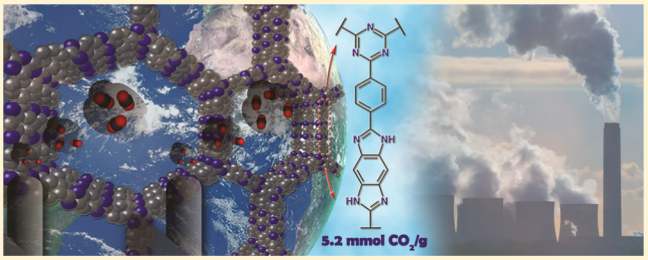


## 1. INTRODUCTION

Over the past two decades porous organic polymers (POPs) received considerable attention due to their potential in gas storage and separation, catalysis, and sensing.[1] The systematic design and diverse synthetic routes of POPs enable the realization of organic polymers exhibiting exceptionally high porosity, remarkable physicochemical stability, and multifunctionality making them highly attractive for a broad range of applications.[2−4] Of particular interest to our research goals is the use of N-rich POPs in selective carbon dioxide ($CO_2$) capture from gas mixtures such as flue, natural, and landfill gases because of the greenhouse nature of $CO_2$.[5,6] $CO_2$ capture and sequestration (CCS) from fossil fuels burning is essential for stabilizing $CO_2$ concentration in the atmosphere until affordable and efficient carbon-free energy sources become widely accessible.[7] The current technology for CCS employs aqueous amine solutions (i.e., MEA, 30% in water) to chemically trap $CO_2$ in the form of carbamate. In spite of its effectiveness, such adsorbents suffer many drawbacks including solvent decomposition and evaporation, toxicity, and corrosiveness in addition to the large energy penalty needed for solvent regeneration.[7] To address these limitations, the use of porous adsorbents like metal−organic frameworks (MOFs) and POPs has been suggested. Unlike amine solutions, porous adsorbents can be tailored to selectively bind $CO_2$ with moderate binding affinities in the physisorption regime to enable regeneration processes with minimal energy cost.[4,8,9] For porous adsorbents, integrating favorable binding sites for $CO_2$ without compromising porosity is essential, as both traits are needed for selective capture and high uptake capacity. As such, N-functionalization of POPs is one of the promising approaches and can be carried out by pre- or postsynthesis modification of POPs. For example, porous aromatic frameworks (PAFs) have been modified by postsynthesis treatment to tether amine functionality into the pore walls or by impregnating with polyethylenimine. In both cases, the modified networks exhibited remarkably increased $CO_2$ uptake and selectivity.[10] Alternatively, condensation reactions can be used to create Lewis basic sites as in the case of benzimidazole-linked polymers (BILPs),[11−15] imine-linked polymers, and Tröger's base-bridged covalent organic polymers (TB-COPs) leading to high $CO_2$ uptake.[16]

Recently, triazine-functionalized POPs were synthesized by incorporating 1,3,5-triazine units into various polymer networks.[17−20] In general, triazine-based POPs exhibit high thermal and chemical stability as well as permanent microporosity.[21−23] Khun et al. reported covalent triazine-based framework (CTF) by trimerization of dicyanobenzene under ionothermal conditions.[17] Subsequently, Cooper and coworkers developed several triazine-based conjugated microporous polymers (TCMPs) which have been synthesized by a palladium-catalyzed Sonogashira−Hagihara cross-coupling reaction.[24] The studies have demonstrated $\pi$-conjugated 1,3,5-triazine core acts as an electron donor and thus enhances $CO_2$−

Received: October 8, 2014
Revised: November 18, 2014
Published: November 26, 2014

   dx.doi.org/10.1021/ma502071w | Macromolecules 2014, 47, 8328−8334

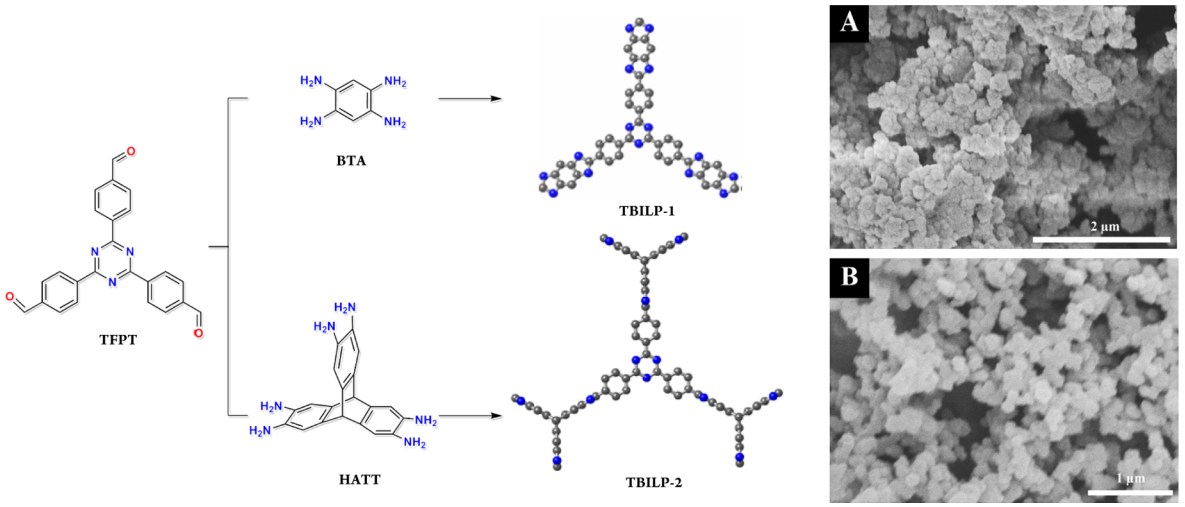


**Figure 1.** Synthesis of TBILPs: (i) DMF, −30 °C, 6 h; (ii) DMF, RT, 6 h under $N_2$; (iii) DMF, 130 °C, 72 h under $O_2$. Scanning electron microscopy (SEM) images of TBILP-1 (A) and TBILP-2 (B).

network interactions. With these considerations in mind, we report on the synthesis of BILPs constructed from triazine-containing building units and assess their potential in $CO_2$ capture from flue gas and methane-rich gases under vacuum swing adsorption (VSA) and pressure swing adsorption (PSA) conditions. The $CO_2$ uptake, selectivity, heat of adsorption, and the $CO_2$ capture performance of TBILPs using a set of $CO_2$ sorbent evaluation criteria suggested by Bae and Snurr[25] were studied.

## 2. EXPERIMENTAL SECTION

**2.1. General Techniques, Materials, and Methods.** All chemicals were purchased from commercial suppliers (Sigma-Aldrich, Acros Organics, and Frontier Scientific) and used without further purification, unless otherwise noted. Air-sensitive samples and reactions were handled under an inert atmosphere of nitrogen using either glovebox or Schlenk line techniques. Chromatographic separations were performed using standard flash column chromatography methods using silica gel purchased from Acros Organics (60 Å, 35−70 $\mu$m). Elemental microanalyses were performed at the Midwest Microlab, LLC. $^1$H and $^{13}$C NMR spectra were obtained on a Varian Mercury-300 MHz. NMR spectrometer. $^{13}$C cross-polarization magic angle spinning (CPMAS) NMR spectra for solid samples were taken at Spectral Data Services, Inc. Thermogravimetric analysis (TGA) was carried out using a TA Instruments Q-5000IR series thermal gravimetric analyzer with samples held in 50 $\mu$L platinum pans under nitrogen (heating rate 10 °C/min). For scanning electron microscopy imaging (SEM), samples were prepared by dispersing the material onto a sticky carbon surface attached to a flat aluminum sample holder. The sample was then coated with platinum at $6 \times 10^{-5}$ mbar for 60 s before imaging. Images were taken on a Hitachi SU-70 scanning electron microscope. Powder X-ray diffraction data were collected on a Panalytical X'pert pro multipurpose diffractometer (MPD). Samples were mounted on a sample holder and measured using Cu K$\alpha$ radiation with a 2$\theta$ range of 1.5−35. FT-IR spectra were obtained as KBr pellets using Nicolet-Nexus 670 spectrometer. Sorption experiments were collected using a Quantachrome Autosorb IQ analyzer. 2,4,6-Tris(4-bromophenyl)-1,3,5-triazine and 2,3,6,7,14,15-hexaaminotriptycene hexahydrochloride were prepared according to literature procedures.[26,17] High-pressure gas sorption measurements were performed by using VTI-HPVA-100 volumetric analyzer. High-pressure total gas uptakes were calculated by reported literature methods, and NIST Thermochemical Properties of Fluid Systems were applied to the calculations.[27]

*Synthesis of 2,4,6-Tris(4-formylphenyl)-1,3,5-triazine (TFPT).* 2,4,6-Tris(4-bromophenyl)-1,3,5-triazine (1.48 g, 2.71 mmol) was dissolved in dry THF (200 mL) under a $N_2$ atmosphere. To the stirred solution, *n*-BuLi was added dropwise (2.5 M in *n*-hexane, 11 mL, 27.5 mmol) at −78 °C. The temperature was allowed to rise to −60 °C and stirred for 3 h. The obtained green solution was treated with anhydrous *N*,*N*-dimethylformamide (DMF) (4.19 mL, 54.2 mmol) at −78 °C. The mixture was stirred overnight, while the temperature was allowed to rise to 25 °C. The milky opaque mixture was acidified with aqueous 3 M HCl (46 mL). The organic volatiles were partially removed by evaporation under reduced pressure, and the product was extracted with $CHCl_3$. The organic phase was washed with water, dried over $MgSO_4$, and filtered. Volatiles were removed under reduced pressure, and the crude light yellow product was further purified by silica gel column using $CHCl_3$ as eluent to afford colorless crystals (800 mg, 74% yield). $^1$H NMR ($CDCl_3$, 300 MHz): $\delta$ (ppm) 10.19 (s, 3H, CHO), 8.95 (d, $J$ = 8.4, 6H, ArH), 8.11 (d, $J$ = 8.1 Hz, 6H, ArH).[28]

**2.2. Synthesis of Polymers.** *Synthesis of TBILP-1.* A 250 mL Schlenk flask was charged with 1,2,4,5-benzenetetramine tetrahydrochloride (64 mg, 0.23 mmol), 65 mL of anhydrous DMF, and a stir bar. The resultant homogeneous solution was cooled to −30 °C and treated dropwise with TFPT (60 mg, 0.152 mmol) dissolved in anhydrous DMF (50 mL). The temperature was maintained around −30 °C for 6 h during which a yellowish-brown solid is formed, and the resultant slurry solution was left to warm to room temperature overnight. The flask containing the reaction mixture was flushed with air for 10 min and capped tightly. The reaction mixture was then transferred to a static oven and heated gradually to 130 °C (0.5 °C/min) and kept for 3 days to afford a fluffy yellow powder. The solid was isolated by filtration over a medium glass frit and subsequently washed with DMF, acetone, water, 0.5 M HCl, 0.5 M NaOH, water, and acetone. The product was then immersed in acetone/chloroform (1:1 v/v) for 1 day, during which the activation solvent was decanted and freshly replenished twice. After filtration, the product was dried at 120 °C under vacuum (150 mTorr) to give TBILP-1 as a fluffy brown powder (50 mg, 81% yield). Anal. Calcd (%) for $C_{34}H_{17}N_4.4H_2O$: C, 75.55; H, 4.37; N, 11.00; Found: C, 73.78; H, 4.52; N, 10.12.

*Synthesis of TBILP-2.* TBILP-2 was prepared according to the method described above for TBILP-1. 2,3,6,7,14,15- Hexaaminotriptycene hexahydrochloride (58 mg, 0.10 mmol) in 90 mL of anhydrous DMF and TFPT (40 mg, 0.10 mmol) in 45 mL of anhydrous DMF were used. After drying, the final product TBILP-2 was obtained as a light brown fluffy solid (45 mg, 79% yield). Anal. Calcd (%) for $C_{68}H_{38}N_8.8H_2O$: C, 74.47; H, 3.97; N,11.32. Found: C, 73.51; H, 4.86; N, 10.09.


dx.doi.org/10.1021/ma502071w | *Macromolecules* 2014, 47, 8328−8334

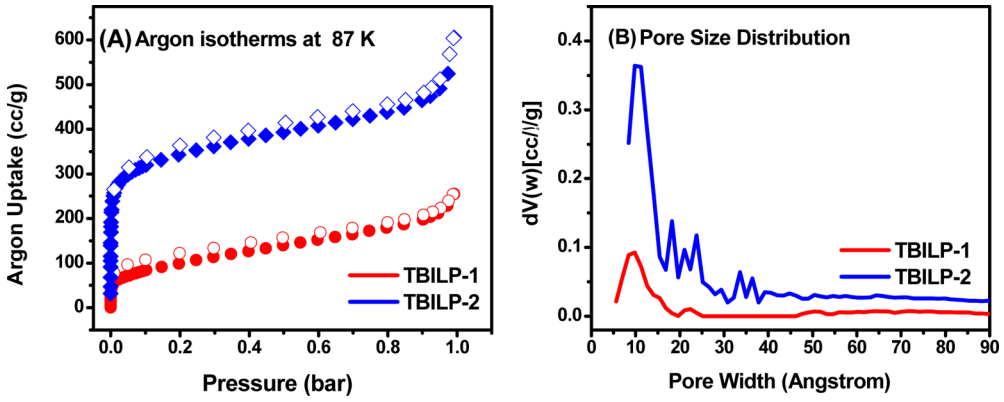


**Figure 2.** (A) Ar uptake isotherms at 87 K and (B) pore size distribution by using NLDFT method. Adsorption (filled) and desorption (empty).

**Table 1. Gas Uptake, Binding Affinity, and Selectivity ($CO_2/N_2$ and $CO_2/CH_4$) for TBILP-1 and TBILP-2**

| | $CO_2$ at 1 bar[a] | | | selectivity[b] | | selectivity[c] | | surface area[d] |
|---|---|---|---|---|---|---|---|---|
| polymer | 273 K | 298 K | $Q_{st}$ | $CO_2/N_2$ | $CO_2/CH_4$ | $CO_2/N_2$ | $CO_2/CH_4$ | BET |
| BILP-5[1] | 128 | 87 | 29 | 36 | 6 | 33 | 5 | 599 |
| BILP-7[1] | 193 | 122 | 28 | 34 | 7 | 32 | 6 | 1122 |
| TBILP-1 | 117 | 78 | 35 | 63 | 9 | 62 | 9 | 330 |
| TBILP-2 | 228 | 146 | 29 | 40 | 7 | 43 | 7 | 1080 |
| TFM-1[2] | 76.1 | N/A | 27 | 29 | N/A | 29 | N/A | 738 |
| TCMP-0[3] | 105 | 59 | N/A | N/A | N/A | N/A | N/A | 963 |
| APOP-1[4] | 188 | 118 | 27 | 20 | 5 | 20 | 5 | 1298 |
| PCTF-1[5] | 145 | 89 | N/A | N/A | N/A | N/A | N/A | 2235 |
| TPI-1[6] | 107 | 55 | 34 | 31 | N/A | 31 | N/A | 809 |

[a]Gas uptake in mg $g^{-1}$ and isosteric enthalpies of adsorption ($Q_{st}$) in kJ $mol^{-1}$ calculated by virial model reported at zero coverage for $CO_2$. [b]Selectivity (mol $mol^{-1}$) was calculated by initial slope method at 298 K. [c]Selectivity (mol $mol^{-1}$) was calculated by IAST method at 298 K. [d]Surface area (BET) in $m^2$ $g^{-1}$.

## 3. RESULTS AND DISCUSSION

In this study, TBILP-1 and TBILP-2 were synthesized by a template-free polycondensation reaction between 2,4,6-tris(4-formylphenyl)-1,3,5-triazine (TFPT) and 1,2,4,5-benzenetetraamine tetrahydrochloride (BTA) and 2,3,6,7,14,15-hexaaminotriptycene hexahydrochloride (HATT), respectively, in good yields (Figure 1). The chemical connectivity of the polymers was investigated by FT-IR and $^{13}C$ CP-MAS NMR, while chemical composition was confirmed by microelemental analysis. The characteristic stretching bands from the imidazole ring were clearly visible in FT-IR spectra at 3415 $cm^{-1}$ due to free N−H and hydrogen-bonded N−H, respectively (Figure S3).[11−15,29] A significant depletion in the intensity of the peak located at 1700 $cm^{-1}$ corresponds to the aldehyde carbonyl, suggests a complete consumption of aldehyde functional groups. The strong absorption band at 1515 $cm^{-1}$ supports the successful incorporation of the 1,3,5-triazine unit in the final polymer network.[17] The $^{13}C$ CP-MAS NMR spectra of TBILPs showed characteristic peaks assigned in Figure S4, representing NC(Ph)N in benzimidazole units.[12] Thermogravimetric analysis (TGA) of as-prepared TBILPs revealed high thermal stability without any decomposition up to 500 °C (Figure S1). The expected amorphous nature of the polymers was established by powder X-ray diffraction studies (Figure S2).

The porosity of the polymers was studied by Ar sorption−desorption isotherms collected at 87 K as shown in Figure 2A. The Brunauer−Emmett−Teller (BET) surface area calculation resulted in values of 330 $m^2$ $g^{-1}$ (TBILP-1) and 1080 $m^2$ $g^{-1}$ (TBILP-2). Ar isotherms were fitted by nonlocal density functional theory (NLDFT) model to calculate pore size distribution (PSD). The dominant PSDs of TBILP-1 and TBILP-2 were found to be centered around 0.92 and 1.1 nm, respectively, (Figure 2B). Pore volumes were calculated at $P/P_0$ = 0.90 and resulted in 0.30 $cm^3$ $g^{-1}$ (TBILP-1) and 0.60 $cm^3$ $g^{-1}$ (TBILP-2). The higher surface area and pore volume of TBILP-2 are most likely attributed to the unique structural features of triptycene core, which has been reported to provide structures of high internal molecular free volume and could probably disfavor the formation of interpenetrated networks.[30,31]

Gas isotherms ($N_2$, $CO_2$, and $CH_4$) were collected at 273 and 298 K to study the gas uptake capacity and selective nature of the polymers. The $CO_2$ uptake of TBILP-2 (5.19 mmol $g^{-1}$/228 mg $g^{-1}$) is much higher than TBILP-1 (2.65 mmol $g^{-1}$/117 mg $g^{-1}$) at 273 K and 1 bar and competes with the best performing porous materials such as ALP-1 (5.37 mmol $g^{-1}$),[32] BILP-4 (5.34 mmol $g^{-1}$),[12] HCPs (3.01−3.92 mmol $g^{-1}$),[33] functionalized CMPs (1.6−1.8 mmol $g^{-1}$),[34] fluorinated FCTFs (4.67−5.53 mmol $g^{-1}$),[19] and PAFs (3.01−3.92 mmol $g^{-1}$).[10] The high $CO_2$ uptake of TBILPs can be attributed to the combined effects of the Lewis basic 1,3,5-triazine and imidazole-building units of the polymers. Consequently, TBILPs revealed improved $CO_2$ uptake compared to their triazine-free BILP analogues. For instance, TBILP-2 (3.32 mmol $g^{-1}$/146 mg $g^{-1}$) showed around 20% more $CO_2$ uptake than BILP-7 (2.77 mmol $g^{-1}$/122 mg $g^{-1}$) at 298 K. Meanwhile, the $CO_2$ uptake of TBILP-1 (1.77 mmol $g^{-1}$/78 mg $g^{-1}$) was comparable with BILP-5 (1.98 mmol $g^{-1}$/87 mg $g^{-1}$) at 298 K and 1 bar, despite the much higher surface area of


dx.doi.org/10.1021/ma502071w | Macromolecules 2014, 47, 8328−8334

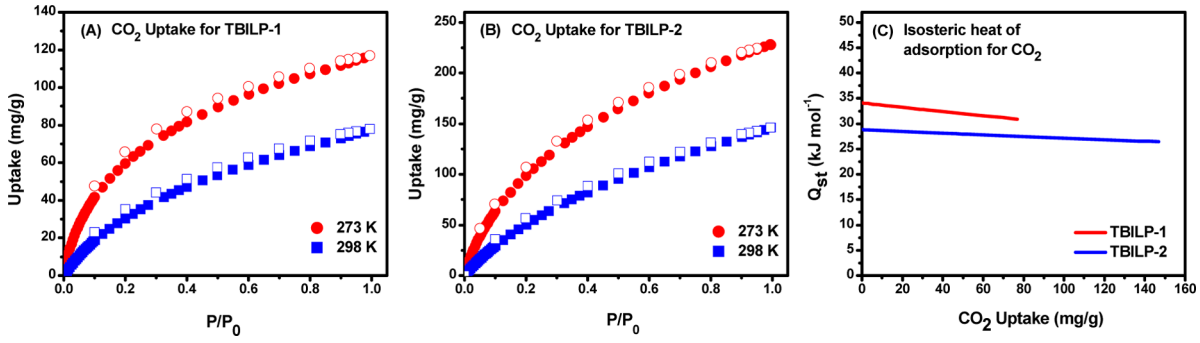


**Figure 3.** $CO_2$ uptake isotherms for TBILP-1 (A) and TBILP-2 (B) at 273 and 298 K and $CO_2$ heats of adsorption calculated by the virial method (C). Adsorption (filled) and desorption (empty).

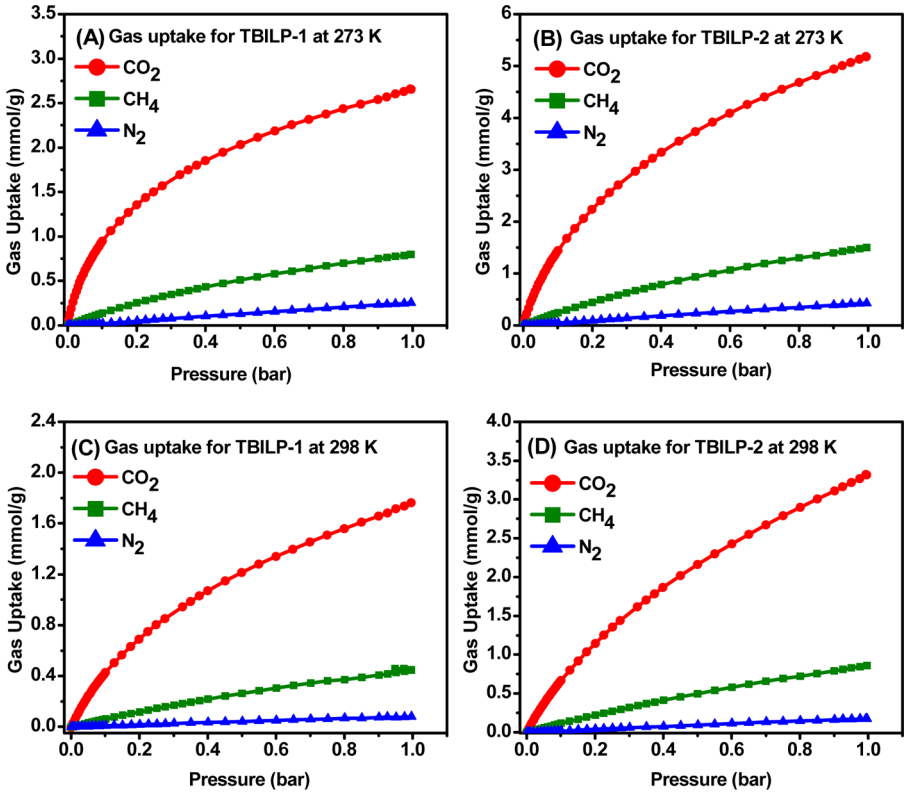


**Figure 4.** $CO_2$, $CH_4$, and $N_2$ gas adsorption isotherms for TBILPs at 273 K (A, B) and 298 K (C, D).

the latter (Table 1). The $CO_2$ uptake of TBILP-1 also competes with triazine-based POPs such as CTFs (0.94−4.17 mmol $g^{-1}$),[18] TCMPs (1.22−2.62 mmol $g^{-1}$),[24] triazine-based polyimide (TPIs) (0.68−2.45 mmol $g^{-1}$),[35] porous covalent triazine frameworks (PCTFs) (1.88−3.31 mmol $g^{-1}$),[36] nanoporous organic polymer (NOP-6) (2.51 mmol $g^{-1}$),[37] and fluorine-based covalent triazine frameworks (*fl*-CTFs) (1.27−4.28 mmol $g^{-1}$).[38] The $CO_2$ uptake at 0.15 bar (partial pressure of $CO_2$ in flue gas) and 298 K was also very high, 0.57 mmol $g^{-1}$ (TBILP-1) and 0.92 mmol $g^{-1}$ (TBILP-2), similar to those of microporous polyimides reported by Li and Wang.[20f] It is very desirable to have high $CO_2$ capacity at this pressure to enhance selective $CO_2$ capture in the presence of other gases as we discuss below.

The $CO_2$ binding affinity is a key parameter for effective adsorbent design. $CO_2$ isosteric heats of adsorption ($Q_{st}$) were calculated by using the virial (Figure 3C) and Clausius−Clapeyron equations. TBILP-1 has a much higher $Q_{st}$ (35 kJ mol$^{-1}$) than TBILP-2 (29 kJ mol$^{-1}$). The difference in $Q_{st}$ values can be reasoned by the pore size distribution of TBILPs, which can play a predominant role in determining the binding affinity of $CO_2$. For instance, while both polymers have the same N-rich building units (i.e., triazine and imidazole), the smaller pores of TBILP-1 can lead to $CO_2$−multipore wall interactions and hence higher $CO_2$ binding affinity. A similar observation was recently reported by Wang et al.; the study highlighted the impact of geometry and metrics of building units on the performance of poly(Schiffbase) networks in selective $CO_2$ capture.[39] The study demonstrated that high surface area and narrow pores lead to high $CO_2$ uptake and selectivity. Both theoretical and experimental studies have revealed that $CO_2$ binding affinity can be enhanced through pore functionalization that enhances adsorbent−$CO_2$ interactions.[40,41] However, such interactions should be maintained in the physisorption regime to facilitate adsorbent regeneration with minimal energy input. It is evident from the $CO_2$


dx.doi.org/10.1021/ma502071w | *Macromolecules* 2014, 47, 8328−8334

isotherms that the binding is fully reversible at 273 and 298 K in spite of the high $Q_{st}$ values (Figure 3C). We have noticed from our recent studies that BILPs in general exhibit desirable $Q_{st}$ values (25−38 kJ mol$^{-1}$) where $CO_2$ can strongly and only physically interact with N-imine functionalities of the polymers.[42] Additional $CO_2$ interactions with aromatic C−H sites were also predicted recently by DFT studies; however, these interactions are considerably lower than those involving the N-imine sites.[15]

Given the high $CO_2$ uptake and desirable binding affinity, we studied the use of TBILPs in selective $CO_2$ capture over $CH_4$ and $N_2$ (Figure 4). The initial steep increase in $CO_2$ uptake can be explained by dipole−quadrupole interactions between $CO_2$ and the N-imine sites of TBILPs. In contrast, both $CH_4$ and $N_2$ adsorption isotherms revealed almost linear correlation between gas uptake and pressure (Figure S7). Henry's law initial slope calculations were applied to single component gas adsorption isotherms at 298 K. TBILP-1 showed high selectivity for $CO_2/N_2$ (63) and $CO_2/CH_4$ (9) at 298 K. The observed selectivity at 298 K for $CO_2/N_2$ (63) of TBILP-1 is the highest among the reported triazine-based POPs and BILPs except BILP-2 (71).[12] As expected, TBILP-2 exhibited relatively lower selectivity for $CO_2/N_2$ (40) and $CO_2/CH_4$ (7) at 298 K, which is most likely due to its larger pores that are more accessible by $CH_4$ and $N_2$. To evaluate the performance of the polymers in $CO_2$ separation from gas mixtures ($CO_2/N_2$ and $CO_2/CH_4$), the Ideal Adsorbed Solutions Theory (IAST) was applied wherein selectivity of binary gas mixtures can be predicted from single component adsorption isotherms as a function of pressure.[45] Two industrial waste gas compositions—postcombustion flue gas and landfill gas—were used to predict selectivity of $CO_2/N_2$ (10/90) and $CO_2/CH_4$ (50/50), respectively. Single component gas adsorption isotherms at 298 K were fitted by either single-site or dual-site Langmuir Fruendlich models. The IAST selectivity results (Figure 5) are in good agreement with those reported above from initial slope selectivity calculations. The gas mixture adsorption behavior of TBILP-1 and TBILP-2 showed high $CO_2/N_2$ selectivity of 62 and 43 at 298 K and $CO_2/CH_4$ selectivity of 9 and 7 at 298 K, respectively.

Furthermore, the promising results of $CO_2$ adsorption and selectivity studies motivated us to follow the set of $CO_2$ capture evaluation criteria proposed by Bae and Snurr to provide a more comprehensive approach for $CO_2$ adsorbent evaluation (Table 2).[25] The criteria include $CO_2$ uptake using single-component gas isotherm ($N_1^{ads}$), working capacity ($\Delta N_1$), regenerability ($R$), selectivity ($\alpha_{12}^{ads}$), and sorbent selection parameter ($S$). The $CO_2$ capture performance of the polymers was evaluated by applying vacuum swing adsorption (VSA) conditions (adsorption at 1 bar and desorption at 0.1 bar) to typical postcombustion flue gas ($CO_2$:$N_2$ = 10:90) and landfill gas ($CO_2$:$CH_4$ = 50:50) compositions. The working capacities of TBILP-1 were found to be 0.35 and 1.02 mol kg$^{-1}$ in the case of flue gas and landfill gas separation, respectively. In contrast, TBILP-2 showed higher $\Delta N_1$ values of 0.59 and 1.84 mol kg$^{-1}$ for flue gas and landfill separation, respectively. The observed $\Delta N_1$ values of TBILP-1 and TBILP-2 are similar to those of ZIF-78, -81, and -82, SNU-Cl-va, UiO-66-AD6, BILPs, and commercial Norit R1 extra.[25,46−48] TBILPs show favorable regenarabilities ($R$ > 80) for both VSA gas separation cases, which point out the reversibility of $CO_2$ adsorption−desorption under ambient conditions. Recent studies also reported that $Q_{st}$ has an inverse correlation with the $R$ factor of polymers.[41]

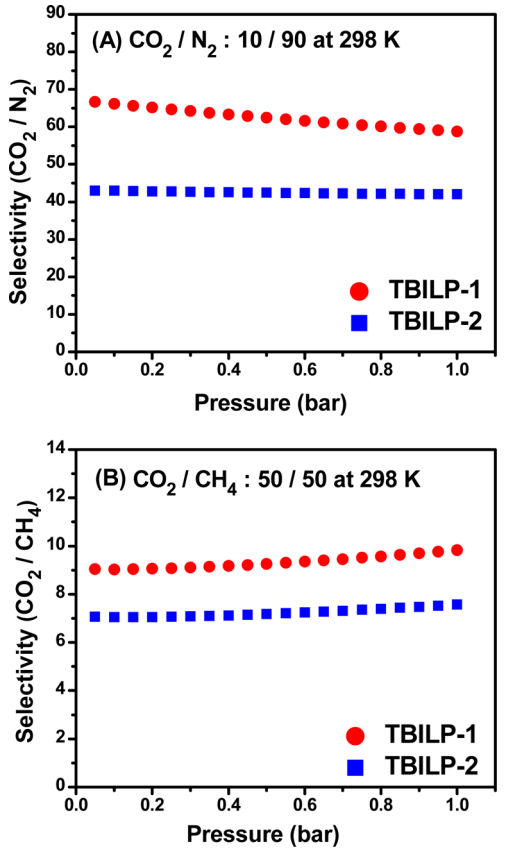


**Figure 5.** IAST selectivity of TBILPs: (A) $CO_2/N_2$ (10/90); (B) $CO_2/CH_4$ (50/50) at 298 K.

**Table 2. $CO_2$ Sorption Evaluation of TBILP by Using Reported Set of Criteria**

| adsorbents | $N_1^{ads}$ (mol kg$^{-1}$) | $\Delta N_1$ (mol kg$^{-1}$) | $R$ | $\alpha_{12}^{ads}$ | $S$ |
|---|---|---|---|---|---|
| VSA in flue gas ($CO_2$:$N_2$ = 10:90) separation at 298 K, $P_{ads}$ = 1 bar, $P_{des}$ = 0.1 bar | | | | | |
| TBILP-1 | 0.40 | 0.35 | 87.0 | 58.7 | 334.6 |
| TBILP-2 | 0.67 | 0.59 | 88.3 | 42.1 | 192.3 |
| VSA in landfill gas ($CO_2$:$CH_4$ = 50:50) separation at 298 K, $P_{ads}$ = 1, $P_{des}$ = 0.1 bar | | | | | |
| TBILP-1 | 1.25 | 1.02 | 81.3 | 9.8 | 107.0 |
| TBILP-2 | 2.20 | 1.84 | 83.7 | 7.6 | 62.5 |
| PSA in landfill gas ($CO_2$:$CH_4$ = 50:50) separation at 298 K, $P_{ads}$ = 5 bar, $P_{des}$ = 1 bar | | | | | |
| TBILP-2 | 4.28 | 2.32 | 54.33 | 7.2 | 31.9 |

Sorbent selection parameter of TBILP-1 (335) in VSA flue gas outperformed all reported porous polymers except ZIF-78 (396), due to the high $CO_2/N_2$ selectivity of TBILP-1. VSA landfill gas and flue gas performance of TBILP-2 also competes with top adsorbent candidates in terms of $S$ factor.

For PSA application, the use of high surface area adsorbents has been suggested to be more effective, and as such, we selected only TBILP-2 for landfill gas separation since TBILP-1 has much lower surface area (330 m$^2$ g$^{-1}$).[41] We collected high-pressure $CO_2$ and $CH_4$ isotherms because PSA operates in a pressure range of 1−5 bar (Table 2). The working capacity of TBILP-2 was calculated to be 2.32 mol kg$^{-1}$, which exceeds the working capacities of Zeolite-13X (1.4 mol kg$^{-1}$), diimide-POP (1.62 mol kg$^{-1}$), and IRMOF-16 (2.18 mol kg$^{-1}$). Notably, the combination of high $CO_2$ working capacity and good $CO_2/CH_4$ selectivity (7.2) of TBILP-2 leads to a remarkably high $S$ factor


dx.doi.org/10.1021/ma502071w | Macromolecules 2014, 47, 8328−8334

(31.9) that is among the highest for reported porous materials in the field.[48]

While the present study uses only single and pure gas isotherms to investigate $CO_2$ uptake and its selective capture from gas mixtures, the presence of humidity may affect both processes. Water adsorption can lead to materials chemical degradation and may compete with $CO_2$ for adsorption sites in some cases. For example, Matzger et al. reported that MOFs having coordinatively unsaturated metal sites (CUMs) loss some of their $CO_2$ uptake when humid conditions are used.[49] According to computational studies, the adsorbed water weakens the CUMs···$CO_2$ interaction and reduces the overall uptake of $CO_2$.[50] However, the adsorbed water still engages in $CO_2$ capture thorough hydrogen bonding although the interaction is weaker than the calculated CUMs···$CO_2$ interactions. Similarly, a recent study on polar microporous organic polymers reported a drop in $CO_2$ uptake under humid conditions; the decrease in the $CO_2$ uptake depended on the nature of the functional polar group.[51] Furthermore, for hydrophobic polymers the $CO_2$ uptake is not affected by humidity. For our TBILPs, the covalent bonding nature between the building units of the polymers makes them exceptionally stable not only toward moisture by also against acids. In fact, all polymers were purified by treatment with 2 M HCl (see Experimental Section), which reflects their high chemical stability. However, because of the hydrophilic nature of the imidazole sites of TBILPs, we anticipate these polymers to provide interaction sites for water and hence may affect the overall $CO_2$ capture and selectivity. Nevertheless, is should be mentioned that upon water uptake by porous materials their affinity for $N_2$ drops considerably, making them more selective for $CO_2/N_2$.[51]

## 4. CONCLUSION

In this study, we have successfully integrated both triazine and benzimidazole building units into porous organic polymers and investigated their impact on $CO_2$ separation from flue and landfill gases. TBILP-2 adsorbs very high $CO_2$ uptake (5.19 mmol $g^{-1}$/228 mg $g^{-1}$) at 1 bar and 273 K. IAST selectivity calculations revealed high $CO_2/N_2$ selectivity of 62 and 43 for TBILP-1 and TBILP-2, respectively, at 298 K. $CO_2/N_2$ selectivity of TBILPs outperforms all triazine-based porous organic polymers reported to date. $CO_2$ heats of adsorption and selectivity studies showed incorporation of triazine units into BILPs could improve selective $CO_2$ adsorption over $N_2$ and $CH_4$. TBILPs also exhibit promising working capacity, regenerability, and sorbent selection parameter values for $CO_2$ capture from flue and landfill gases under VSA and PSA processes, making them attractive candidates for use in $CO_2$ capture and separation applications.

## ■ ASSOCIATED CONTENT

### Supporting Information

Spectral characterization of polymers and their gas uptake and selectivity studies. This material is available free of charge via the Internet at http://pubs.acs.org.

## ■ AUTHOR INFORMATION

### Corresponding Author

*Fax (804) 828-8599; Tel (804) 828-7505; e-mail helkaderi@vcu.edu (H.M.E-K.).

### Notes

The authors declare no competing financial interest.

## ■ ACKNOWLEDGMENTS

Research supported by the U.S. Department of Energy, Office of Basic Energy Sciences, under Award DE-SC0002576. S.A. thanks Tafila Technical University for fellowship. T.İ. thanks the Ministry of National Education of Turkey for a fellowship.

## ■ REFERENCES

(1) Ding, S.-Y.; Wang, W. *Chem. Soc. Rev.* **2013**, *42*, 548.
(2) Xu, Y.; Jin, S.; Xu, H.; Nagai, A.; Jiang, D. *Chem. Soc. Rev.* **2013**, *42*, 8012.
(3) Chang, Z.; Zhang, D.-S.; Chen, Q.; Bu, X.-H. *Phys. Chem. Chem. Phys.* **2013**, *15*, 5430.
(4) Dawson, R.; Cooper, A. I.; Adams, D. J. *Prog. Polym. Sci.* **2012**, *37*, 530.
(5) Dawson, R.; Stockel, E.; Holst, J. R.; Adams, D. J.; Cooper, A. I. *Energy Environ. Sci.* **2011**, *4*, 4239.
(6) Li, P. Z.; Zhao, Y. L. *Chem.—Asian J.* **2013**, *8*, 1680.
(7) Haszeldine, R. S. *Science* **2009**, *325*, 1647.
(8) D'alessandro, D. M.; Smit, B.; Long, J. R. *Angew. Chem., Int. Ed.* **2010**, *49*, 6058.
(9) Sumida, K.; Rogow, D. L.; Mason, J. A.; McDonald, T. M.; Bloch, E. D.; Herm, Z. R.; Bae, T.-H.; Long, J. R. *Chem. Rev.* **2011**, *112*, 724.
(10) Sung, S.; Suh, M. P. *J. Mater. Chem. A* **2014**, *2*, 13245.
(11) Rabbani, M. G.; El-Kaderi, H. M. *Chem. Mater.* **2011**, *23*, 1650.
(12) Rabbani, M. G.; El-Kaderi, H. M. *Chem. Mater.* **2012**, *24*, 1511.
(13) Rabbani, M. G.; Reich, T. E.; Kassab, R. M.; Jackson, K. T.; El-Kaderi, H. M. *Chem. Commun.* **2012**, *48*, 1141.
(14) Rabbani, M. G.; Sekizkardes, A. K.; El-Kadri, O. M.; Kaafarani, B. R.; El-Kaderi, H. M. *J. Mater. Chem.* **2012**, *22*, 25409.
(15) Altarawneh, S.; Behera, S.; Jena, P.; El-Kaderi, H. M. *Chem. Commun.* **2014**, *50*, 3571.
(16) (a) Zhu, X.; Do-Thanh, C.-L.; Murdock, C. R.; Nelson, K. M.; Tian, C.; Brown, S.; Mahurin, S. M.; Jenkins, D. M.; Hu, J.; Zhao, B.; Liu, H.; Dai, S. *ACS Macro Lett.* **2013**, *2*, 660. (b) Byun, J.; Je, S.-H.; Patel, H. A.; Coskun, A.; Yavuz, C. T. *J. Mater. Chem. A* **2014**, *2*, 12507.
(17) Kuhn, P.; Antonietti, M.; Thomas, A. *Angew. Chem., Int. Ed.* **2008**, *47*, 3450.
(18) Ren, S. J.; Bojdys, M. J.; Dawson, R.; Laybourn, A.; Khimyak, Y. Z.; Adams, D. J.; Cooper, A. I. *Adv. Mater.* **2012**, *24*, 2357.
(19) Zhao, Y.; Yao, K. X.; Teng, B.; Zhang, T.; Han, Y. *Energy Environ. Sci.* **2013**, *6*, 3684.
(20) (a) Bojdys, M. J.; Jeromenok, J.; Thomas, A.; Antonietti, M. *Adv. Mater.* **2010**, *22*, 2202. (b) Zou, X. Q.; Ren, H.; Zhu, G. S. *Chem. Commun.* **2013**, *49*, 3925. (c) Zhu, X.; Mahurin, S. M.; An, S.-H.; Do-Thanh, C.-L.; Tian, C.; Li, Y.; Gill, L. W.; Hagaman, E. W.; Bian, Z.; Zhou, J.-H.; Hu, J.; Liu, H.; Dai, S. *Chem. Commun.* **2014**, *50*, 7933. (d) Wu, S.; Liu, Y.; Guan, G. J.; Pan, C.; Du, Y.; Xiong, X.; Wang, Z. *Macromolecules* **2014**, *47*, 2875. (e) Shen, C.; Yu, H.; Wang, Z. *Chem. Commun.* **2014**, *50*, 11238. (f) Li, G.; Zhang, B.; Yan, J.; Wang, Z. *Macromolecules* **2014**, *47*, 6664.
(21) Kuhn, P.; Forget, A.; Su, D.; Thomas, A.; Antonietti, M. *J. Am. Chem. Soc.* **2008**, *130*, 13333.
(22) Kuhn, P.; Thomas, A.; Antonietti, M. *Macromolecules* **2008**, *42*, 319.
(23) Katekomol, P.; Roeser, J.; Bojdys, M.; Weber, J.; Thomas, A. *Chem. Mater.* **2013**, *25*, 1542.
(24) Ren, S.; Dawson, R.; Laybourn, A.; Jiang, J. X.; Khimyak, Y.; Adams, D. J.; Cooper, A. I. *Polym. Chem.* **2012**, *3*, 928.
(25) Bae, Y. S.; Snurr, R. Q. *Angew. Chem., Int. Ed.* **2011**, *50*, 11586.
(26) Ranganathan, A.; Heisen, B. C.; Dix, I.; Meyer, F. *Chem. Commun.* **2007**, 3637.
(27) Ma, S. Q.; Zhou, H. C. *Chem. Commun.* **2010**, *46*, 44.
(28) Li, S.-H.; Huang, H.-P.; Yu, S.-Y.; Li, X.-P. *Chin. J. Chem.* **2006**, *24*, 1225.

(29) Lee, H. Y.; Park, J.; Lah, M. S.; Hong, J. I. *Chem. Commun.* **2007**, 5013.
(30) Kahveci, Z.; Islamoglu, T.; Shar, G. A.; Ding, R.; El-Kaderi, H. M. *CrystEngComm* **2013**, *15*, 1524.
(31) Prasad, T. K.; Suh, M. P. *Chem.—Eur. J.* **2012**, *18*, 8673.
(32) Arab, P.; Rabbani, M. G.; Sekizkardes, A. K.; İslamoğlu, T.; El-Kaderi, H. M. *Chem. Mater.* **2014**, *26*, 1385.
(33) Martin, C. F.; Stockel, E.; Clowes, R.; Adams, D. J.; Cooper, A. I.; Pis, J. J.; Rubiera, F.; Pevida, C. *J. Mater. Chem.* **2011**, *21*, 5475.
(34) Dawson, R.; Adams, D. J.; Cooper, A. I. *Chem. Sci.* **2011**, *2*, 1173.
(35) Liebl, M. R.; Senker. *Chem. Mater.* **2013**, *25*, 970.
(36) Bhunia, A.; Vasylyeva, V.; Janiak, C. *Chem. Commun.* **2013**, *49*, 3961.
(37) Xiong, S.; Fu, X.; Xiang, L.; Yu, G.; Guan, J.; Wang, Z.; Du, Y.; Xiong, X.; Pan, C. *Polym. Chem.* **2014**, *5*, 3424.
(38) Hug, S.; Mesch, M. B.; Oh, H.; Popp, N.; Hirscher, M.; Senker, J.; Lotsch, B. V. *J. Mater. Chem. A* **2014**, *2*, 5928.
(39) Li, G.; Zhang, B.; Yan, J.; Wang, Z. *Chem. Commun.* **2014**, *50*, 1897.
(40) (a) Dawson, R.; Cooper, A. I.; Adams, D. J. *Polym. Int.* **2013**, *62*, 345. (b) İslamoğlu, T.; Rabbani, M. G.; El-Kaderi, H. M. *J. Mater. Chem. A* **2013**, *1*, 10259.
(41) Wilmer, C. E.; Farha, O. K.; Bae, Y. S.; Hupp, J. T.; Snurr, R. Q. *Energy Environ. Sci.* **2012**, *5*, 9849.
(42) Nugent, P.; Belmabkhout, Y.; Burd, S. D.; Cairns, A. J.; Luebke, R.; Forrest, K.; Pham, T.; Ma, S. Q.; Space, B.; Wojtas, L.; Eddaoudi, M.; Zaworotko, M. J. *Nature* **2013**, *495*, 80.
(43) Zhu, X.; Tian, C.; Mahurin, S. M.; Chai, S.-H.; Wang, C.; Brown, S.; Veith, G. M.; Luo, H.; Liu, H.; Dai, S. *J. Am. Chem. Soc.* **2012**, *134*, 10478.
(44) Song, W.-C.; Xu, X.-K.; Chen, Q.; Zhuang, Z.-Z.; Bu, X.-H. *Polym. Chem.* **2013**, *4*, 4690.
(45) Myers, A. L.; Prausnitz, J. M. *AIChE J.* **1965**, *11*, 121.
(46) Xie, L. H.; Suh, M. P. *Chem.—Eur. J.* **2013**, *19*, 11590.
(47) Hong, D. H.; Suh, M. P. *Chem.—Eur. J.* **2014**, *20*, 426.
(48) Sekizkardes, A. K.; Islamoglu, T.; Kahveci, Z.; El-Kaderi, H. M. *J. Mater. Chem. A* **2014**, *2*, 12492.
(49) Kizzie, A. C.; Wong-Foy, A. G.; Matzger, A. J. *Langmuir* **2011**, *27*, 6368.
(50) Yu, J.; Balbuena, P. B. *J. Phys. Chem. C* **2013**, *117*, 3383.
(51) Woodward, R. T.; Stevens, L. A.; Dawson, R.; Vijayaraghavan, M.; Hasell, T.; Silverwood, I. P.; Ewing, A. V.; Ratvijitvech, T.; Exley, J. D.; Chong, S. Y.; Blanc, F.; Adams, D. J.; Kazarian, S. G.; Snape, C. E.; Drage, T. C.; Cooper, A. I. *J. Am. Chem. Soc.* **2014**, *136*, 9028.